# High-dimensional analysis reveals a pathogenic role of inflammatory monocytes in experimental diffuse alveolar hemorrhage

Lee and Nelson-Maney et al.

## Supplemental Tables

Supplemental Table 1. Listing of antibodies used for mass cytometry and flow cytometry

Supplemental Table 2. Gene set enrichment analysis of monocytes and macrophages in DAH

Supplemental Table 3. Gene set enrichment analysis of peritoneal exudate cells in pristane-treated WT vs. Irf8$^{-/-}$ mice by RNAseq

## Supplemental Figures

Supplemental Figure 1. DAH in mouse strains with defects in innate immunity and gating strategy for mass cytometry analysis.

Supplemental Figure 2. Massive cytometry analysis of lung immune cells in DAH

Supplemental Figure 3. Characterization of neutrophils and monocytes in pristane-induced DAH.

Supplemental Figure 4. scRNAseq analysis of lung immune cells in DAH

Supplemental Figure 5. Irf8 is required for the development of pristane-induced DAH.

Supplemental Figure 6. Irf8 is required for the development of pristane-induced autoimmunity

Supplemental Figure 7. Attenuated DAH in mice deficient of Ccr2 or Cx3cr1

**Supplemental Table 1.** List of antibodies used for mass cytometry and flow cytometry

| Antibody | Clone | Metal conjugate | Fluorophore conjugate |
|---|---|---|---|
| CCR2 | SA203G11 | 174Yb | APC |
| CD103 | 2E7 | 154Sm | |
| CD115 | AFS98 | 142Nd | |
| CD11b | M1/70 | 169Tm | PB |
| CD11c | N418 | 146Nd | APC |
| CD14 | Sa14-2 | 156Gd | |
| CD19 | 6D5 | 149Sm | |
| CD21 | 7E9 | 143Nd | |
| CD24 | M1/69 | 162Dy | |
| CD3 | 145-2C11 | 152Sm | |
| CD4 | RM4-5 | 145Nd | |
| CD44 | IM7 | 141Pr | |
| CD45 | 30-F11 | 165Ho | FITC ,PB |
| CD64 | x54-5/7.1 | 168Er | |
| CD68 | FA-11 | 155Gd | |
| CD69 | H1.2F3 | 173Yb | |
| CD8a | 53-6.7 | 164Dy | |
| CX3CR1 | SA011F11 | 150Nd | PE |
| F4/80 | BM8 | 175Lu | |
| Ly6C | HK1.4 | 151Eu | PECy7 |
| Ly6G | 1A8 | 158Gd | FITC, APCCy7 |
| MHC II | M5/114.15.2 | 209Bi | |
| NK1.1 | PK136 | 163Dy | |
| PDCA-1 | 927 | 148Nd | |
| Siglec F (CD170) | E50-2440 | 170Er | PE |

* PE: phycoerythrin; PB: Pacific Blue; APC: Allophycocyanin; FITC: Fluorescein isothiocyanate; AF: Alexa Fluor; Cy7: Cyanine 7.

**Supplemental Table 2.** Gene set enrichment analysis of monocyte subsets in DAH*

Ly6C$^{hi}$ monocyte

| Upregulated in Pristane | SIZE | ES | NES | NOM p-val | FDR q-val | FWER p-val |
|---|---|---|---|---|---|---|
| HALLMARK_TNFA_SIGNALING_VIA_NFKB | 78 | -0.500 | -1.736 | 0.000 | 0.118 | 0.097 |
| HALLMARK_IL6_JAK_STAT3_SIGNALING | 27 | -0.603 | -1.717 | 0.009 | 0.076 | 0.120 |
| HALLMARK_KRAS_SIGNALING_UP | 30 | -0.586 | -1.704 | 0.009 | 0.059 | 0.138 |
| HALLMARK_ESTROGEN_RESPONSE_LATE | 20 | -0.643 | -1.695 | 0.010 | 0.049 | 0.151 |
| HALLMARK_GLYCOLYSIS | 17 | -0.655 | -1.651 | 0.016 | 0.062 | 0.226 |
| HALLMARK_INFLAMMATORY_RESPONSE | 44 | -0.458 | -1.452 | 0.039 | 0.251 | 0.726 |
| Upregulated in PBS | | | | | | |
| HALLMARK_ADIPOGENESIS | 29 | 0.459 | 1.514 | 0.031 | 0.235 | 0.316 |

Ly6C$^{lo}$ monocyte

| Upregulated in Pristane | SIZE | ES | NES | NOM p-val | FDR q-val | FWER p-val |
|---|---|---|---|---|---|---|
| HALLMARK_INFLAMMATORY_RESPONSE | 44 | -0.620 | -2.126 | 0.000 | 0.000 | 0.000 |
| HALLMARK_TNFA_SIGNALING_VIA_NFKB | 78 | -0.516 | -1.974 | 0.000 | 0.003 | 0.004 |
| HALLMARK_KRAS_SIGNALING_UP | 30 | -0.535 | -1.686 | 0.011 | 0.070 | 0.132 |
| HALLMARK_ESTROGEN_RESPONSE_LATE | 20 | -0.572 | -1.677 | 0.013 | 0.060 | 0.149 |
| HALLMARK_REACTIVE_OXIGEN_SPECIES | 15 | -0.596 | -1.608 | 0.024 | 0.083 | 0.237 |
| HALLMARK_COMPLEMENT | 44 | -0.448 | -1.567 | 0.013 | 0.096 | 0.320 |
| HALLMARK_MTORC1_SIGNALING | 53 | -0.395 | -1.417 | 0.041 | 0.203 | 0.669 |
| Upregulated in PBS | | | | | | |
| HALLMARK_MYC_TARGETS_V1 | 47 | 0.411 | 1.480 | 0.050 | 0.271 | 0.494 |

Alveolar macrophage

| Upregulated in Pristane | SIZE | ES | NES | NOM p-val | FDR q-val | FWER p-val |
|---|---|---|---|---|---|---|
| HALLMARK_INFLAMMATORY_RESPONSE | 44 | -0.541 | -1.831 | 0.000 | 0.041 | 0.032 |
| HALLMARK_COMPLEMENT | 44 | -0.499 | -1.669 | 0.006 | 0.114 | 0.173 |
| HALLMARK_COAGULATION | 22 | -0.549 | -1.613 | 0.023 | 0.138 | 0.297 |
| HALLMARK_CHOLESTEROL_HOMEOSTASIS | 16 | -0.596 | -1.598 | 0.025 | 0.119 | 0.332 |
| Upregulated in PBS | | | | | | |
| None | | | | | | |

## Neutrophil

| Upregulated in Pristane | SIZE | ES | NES | NOM p-val | FDR q-val | FWER p-val |
|---|---|---|---|---|---|---|
| HALLMARK_INTERFERON_GAMMA_RESPONSE | 22 | -0.848 | -2.293 | 0.000 | 0.000 | 0.000 |
| HALLMARK_INFLAMMATORY_RESPONSE | 29 | -0.679 | -1.971 | 0.000 | 0.000 | 0.001 |
| HALLMARK_TNFA_SIGNALING_VIA_NFKB | 59 | -0.547 | -1.830 | 0.000 | 0.012 | 0.021 |
| HALLMARK_APOPTOSIS | 53 | -0.552 | -1.655 | 0.015 | 0.042 | 0.101 |

Upregulated in PBS

None

*pathways were filtered based on nominal p-value < 0.05

**Supplemental Table 3.** Gene set enrichment analysis of peritoneal exudate cells in pristane-treated WT vs. Irf8-/- mice by RNAseq*

| Upregulated in WT | SIZE | ES | NES | NOM p-val | FDR q-val | FWER p-val |
|---|---|---|---|---|---|---|
| HALLMARK_INTERFERON_ALPHA_RESPONSE | 74 | 0.784 | 2.631 | 0.000 | 0.000 | 0.000 |
| HALLMARK_INTERFERON_GAMMA_RESPONSE | 162 | 0.637 | 2.363 | 0.000 | 0.000 | 0.000 |
| HALLMARK_ALLOGRAFT_REJECTION | 151 | 0.542 | 2.012 | 0.000 | 0.000 | 0.000 |
| HALLMARK_INFLAMMATORY_RESPONSE | 148 | 0.525 | 1.961 | 0.000 | 0.000 | 0.000 |
| HALLMARK_TNFA_SIGNALING_VIA_NFKB | 165 | 0.458 | 1.719 | 0.000 | 0.005 | 0.029 |
| HALLMARK_HEDGEHOG_SIGNALING | 18 | 0.678 | 1.665 | 0.005 | 0.009 | 0.062 |
| HALLMARK_CHOLESTEROL_HOMEOSTASIS | 56 | 0.488 | 1.564 | 0.014 | 0.021 | 0.165 |

| Upregulated in $Irf8^{-/-}$ | SIZE | ES | NES | NOM p-val | FDR q-val | FWER p-val |
|---|---|---|---|---|---|---|
| HALLMARK_E2F_TARGETS | 158 | -0.695 | -2.762 | 0.000 | 0.000 | 0.000 |
| HALLMARK_G2M_CHECKPOINT | 149 | -0.627 | -2.452 | 0.000 | 0.000 | 0.000 |
| HALLMARK_SPERMATOGENESIS | 45 | -0.547 | -1.749 | 0.000 | 0.007 | 0.016 |
| HALLMARK_DNA_REPAIR | 126 | -0.437 | -1.670 | 0.000 | 0.015 | 0.048 |
| HALLMARK_MITOTIC_SPINDLE | 155 | -0.381 | -1.500 | 0.005 | 0.060 | 0.219 |

*pathways were filtered based on nominal p-value < 0.05

Supplemental Figure 1

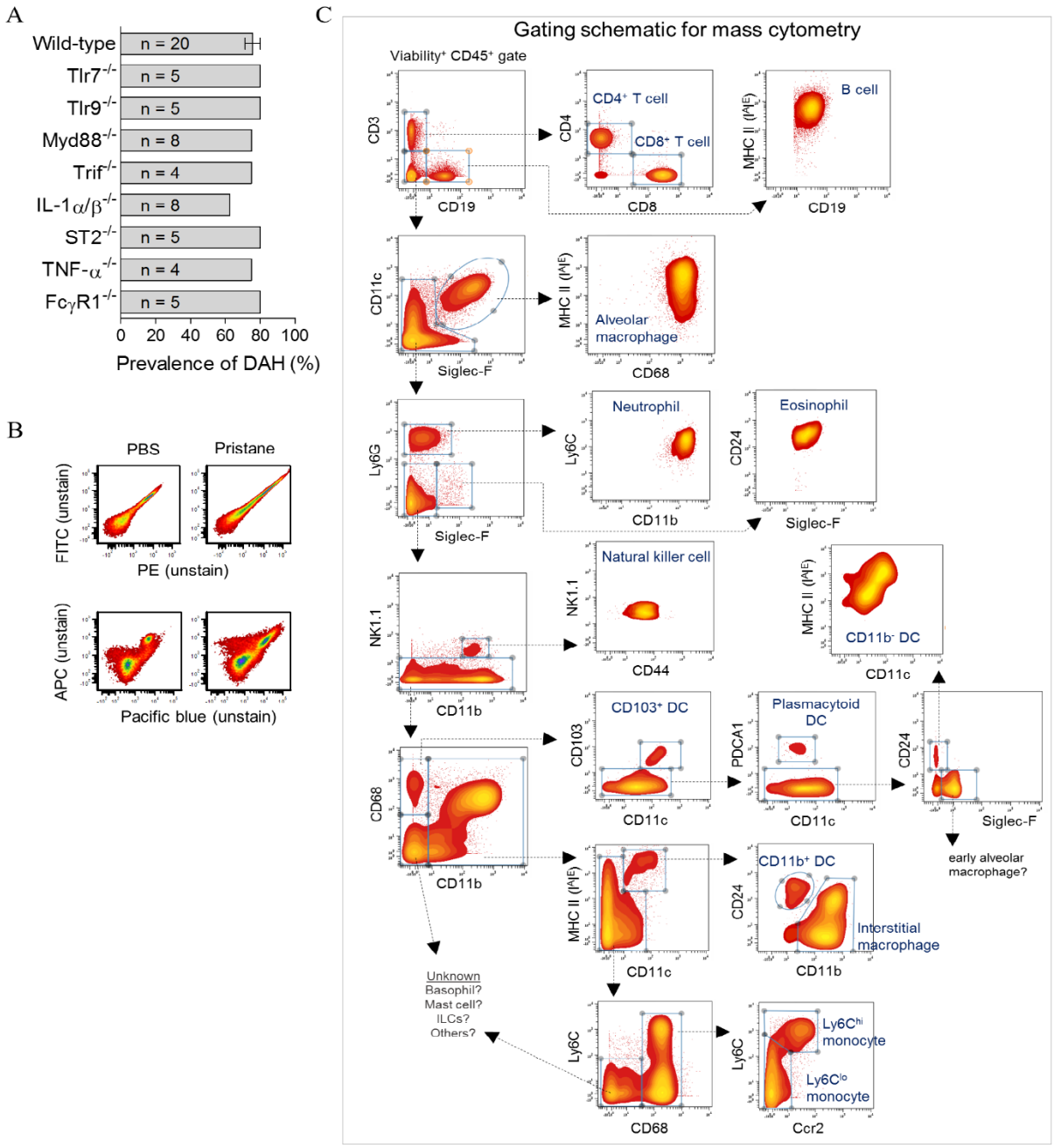


**Supplemental Figure 1. DAH in mouse strains with defects in innate immunity and gating strategy for mass cytometry analysis.** A) Prevalence of pristane-induced DAH in mice with defective TLR signaling components (Tlr7, Tlr9, Myd88 and Trif), IL-1α/β, ST2 (receptor for IL-33), TNFα or Fc receptor γ chain. The prevalence in the wildtype group represents the average of 4 independent experiments with n = 5 per experiment. B) Flow cytometry analysis of unstained isolated cells from digested lung tissue of PBS- or pristane-treated mice (live cell gate). C) Gating strategy for mass cytometry analysis of isolated cells from digested lung tissue.

Supplemental Figure 2

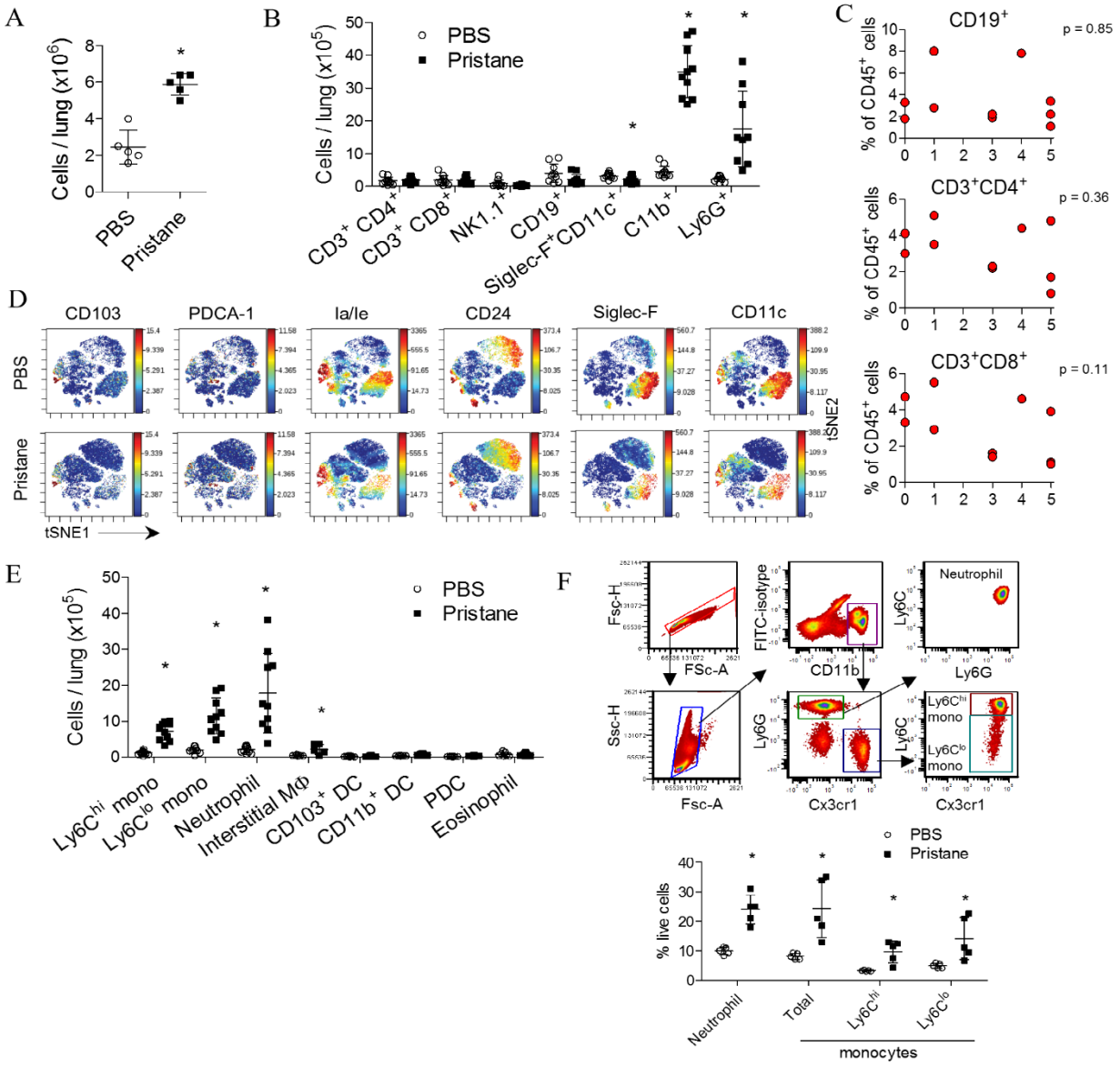


**Supplemental Figure 2. Mass cytometry analysis of lung immune cells in DAH.** A) Total cell count from the digested right lung of mice 2 weeks after PBS or pristane treatment (n = 5 per group). B) Absolute count of lung cell populations from mass cytometry analysis (n = 10 per group). C) Correlation of lung lymphocyte populations with DAH severity score (n = 10). D) viSNE display of dendritic cell markers from mass cytometry analysis of digested lung tissue. E) Absolute count of non-lymphoid cells (CD45+CD3-CD19- gate) in the digested lung tissue of PBS- or pristane-treated mice (n = 10 per group). F) Gating strategy and quantification of lung monocyte and neutrophil by flow cytometry (n = 4 per group). Data are representative of 3 independent experiments (panels A, D, F) or pooled from 2 independent experiments (panel B, C, E). * Statistical analysis was performed using unpaired Student's t-test (panels A, B, E). $p < 0.05$

Supplemental Figure 3

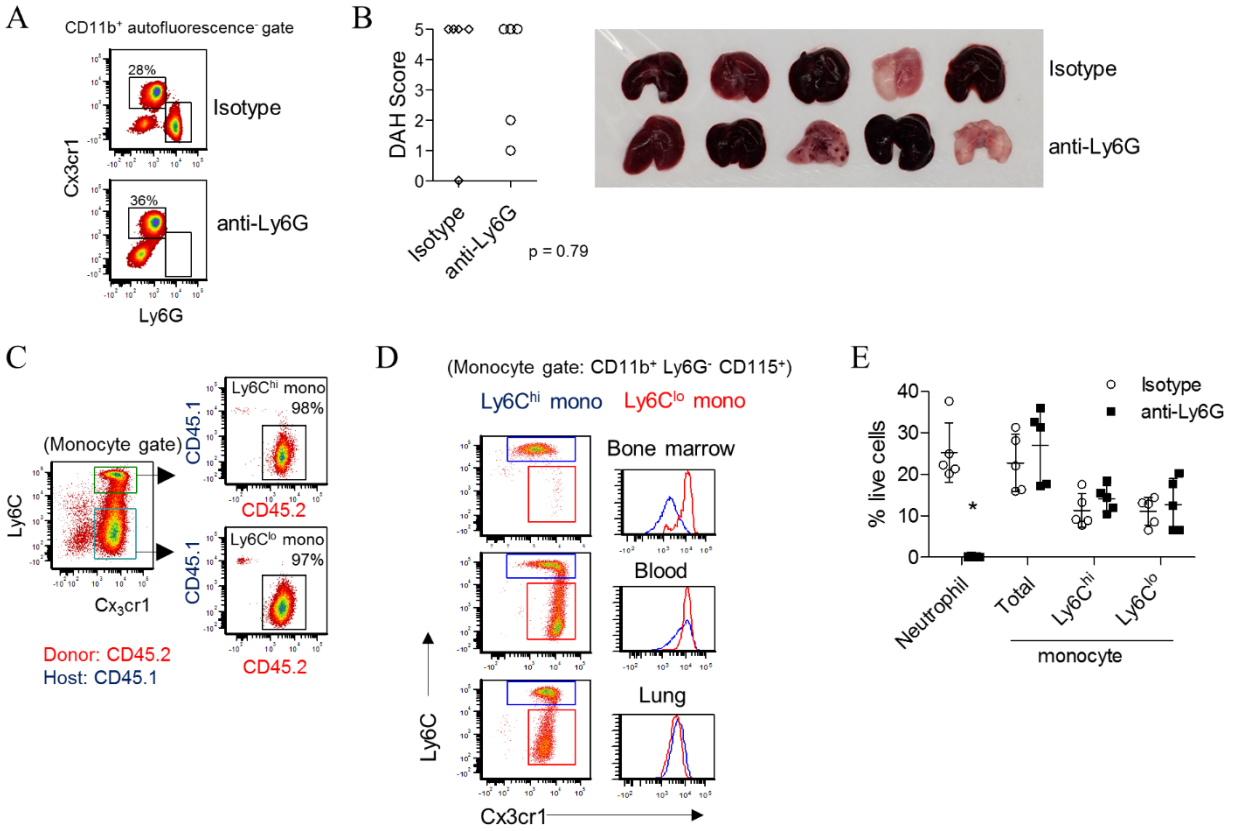


**Supplemental Figure 3. Characterization of neutrophils and monocytes in pristane-induced DAH.** A) Representative flow cytometry plot illustrating lung neutrophil depletion by anti-Ly6G antibodies. B) Quantification and gross illustration of DAH severity in pristane-treated mice treated with isotype or anti-Ly6G antibodies (n = 5 per group). C) Flow cytometry analysis of lung monocytes to discriminate host origin (CD45.1) vs. donor origin (CD45.2) 4 weeks after bone marrow transplant. D) Comparison of Cx3cr1 staining on monocyte subsets in the bone marrow, peripheral blood, and lungs of pristane-treated mice by flow cytometry. E) Flow cytometry analysis of monocyte and neutrophil populations in pristane-treated mice treated with isotype or anti-Ly6G antibodies every 2 days for 2 weeks. Data are representative of 5 or more samples for each experiments (panels A, C, D). Statistical analysis was performed using unpaired Student's t-test (panels B, E). * $p < 0.05$

Supplemental Figure 4

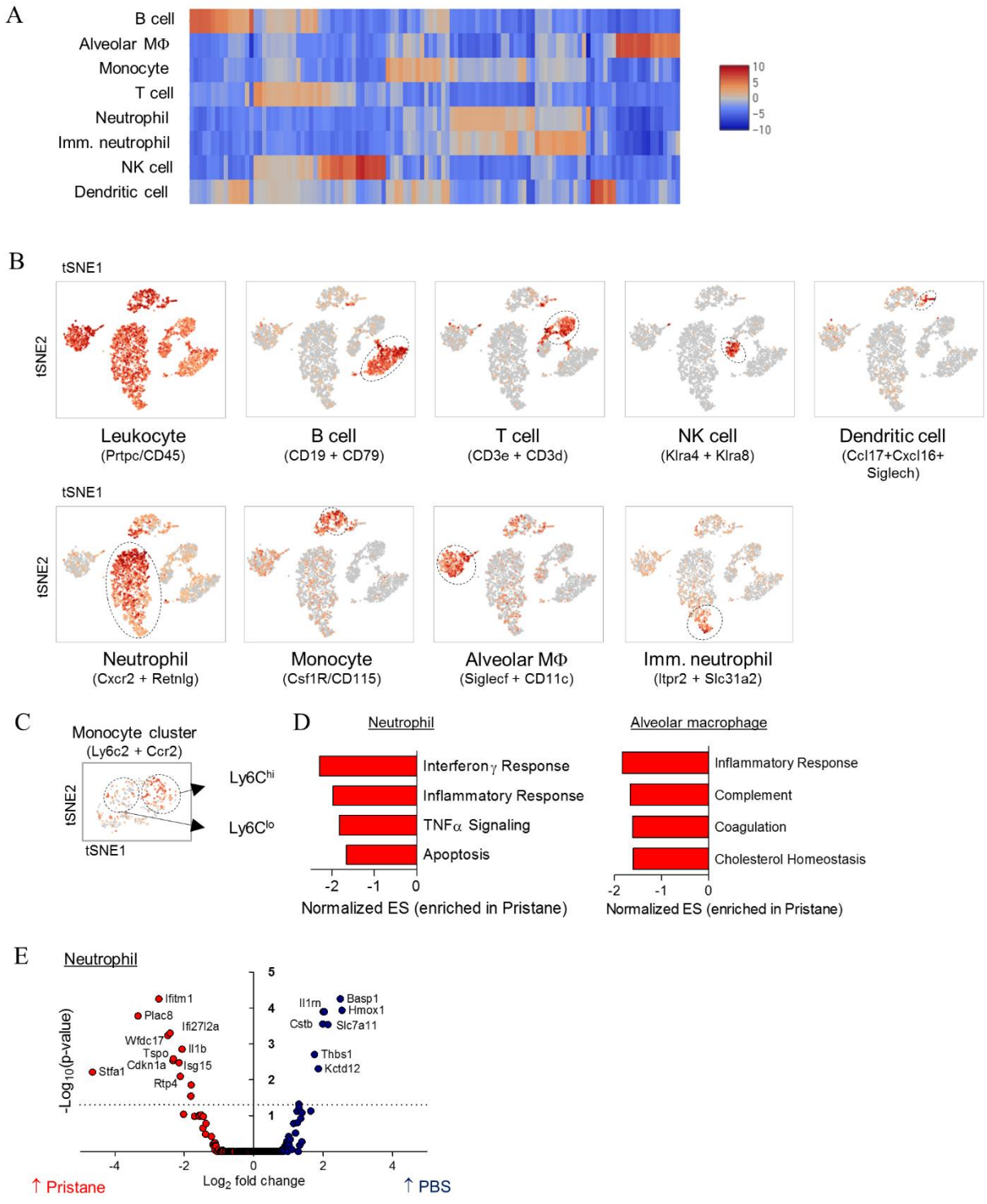


**Supplemental Figure 4. scRNAseq analysis of lung immune cells in DAH.** A) Heat map display of differentially expressed genes in lung lymphoid and myeloid populations. B) viSNE display of individual or combined lineage identifying markers for each immune cell population.

C) Distinction of monocyte subsets based on the expression of Ly6C and Ccr2 on viSNE plot. D) GSEA of lung neutrophils alveolar macrophages in PBS- vs. pristane-treated mice. Gene sets with significant enrichment ($p < 0.05$; FDR < 0.10) after pristane treatment were ranked by the normalized enrichment score. E) Illustration of differentially regulated genes in lung neutrophils of mice treated with PBS vs. pristane.

Supplemental Figure 5

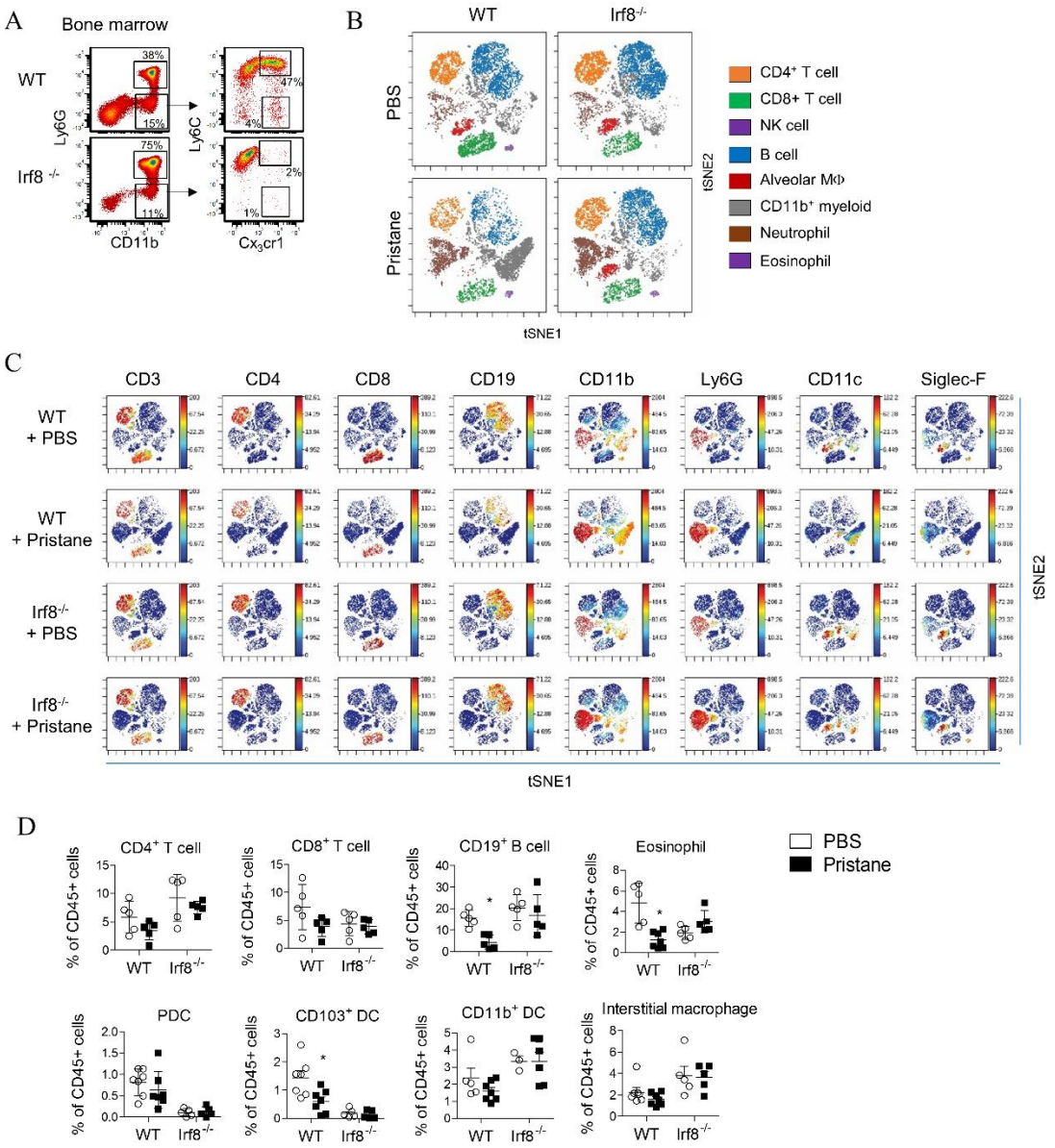


**Supplemental Figure 5. Irf8 is required for the development of pristane-induced DAH.** A) Flow cytometry plot of bone marrow monocytes in WT and Irf8$^{-/-}$ mice. CD11b$^{+}$Ly6G$^{+}$: neutrophil gate. CD11b$^{+}$Ly6G$^{-}$Cx3cr1$^{+}$: monocyte gate. B) viSNE display of lung immune cells (CD45$^{+}$ gate) from pristane-treated WT vs. Irf8$^{-/-}$ mice (n = 5 mice per group) by cell population identity and C) by individual lineage identification markers using mass cytometry. D) Quantitative comparison of lung immune cell populations (CD45$^{+}$ gate) from pristane-treated WT vs. Irf8$^{-/-}$ mice (n = 5-8 per group) from mass cytometry analysis. Data are representative of 2 or more independent experiments. * $p < 0.05$

Supplemental Figure 6

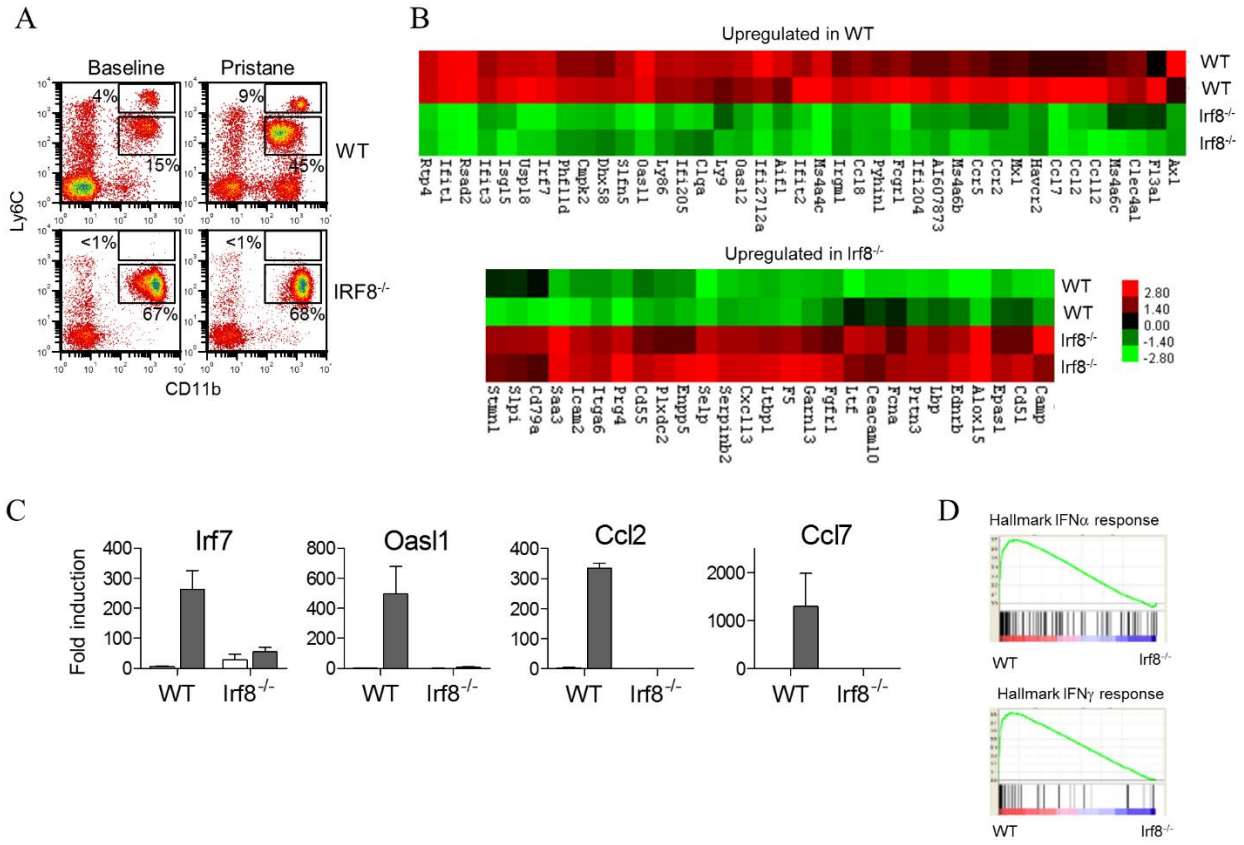


**Supplemental Figure 6. Irf8 is required for the development of pristane-induced autoimmunity**. A) Flow cytometry plot of peripheral blood monocytes and neutrophils in WT and Irf8$^{-/-}$ mice in response to pristane treatment (n = 4 per group). Upper gate box indicates Ly6C$^{hi}$ monocytes while lower gate box indicates Ly6C$^{int}$ Ly6G$^{+}$ neutrophils. B) Heat map of differentially regulated genes in PEC from WT and Irf8$^{-/-}$ mice two weeks after pristane treatment. Genes were filtered based on $Log_2$ fold difference of 4 or greater. C) qPCR confirmation of interferon-stimulated gene expression in PEC from pristane treated WT and Irf8$^{-/-}$ mice (n = 4 per group). D) GSEA plot illustrating enrichment of IFN signature in WT mice compared to Irf8$^{-/-}$ mice. Data are representative of 2 or more independent experiments.

Supplemental Figure 7

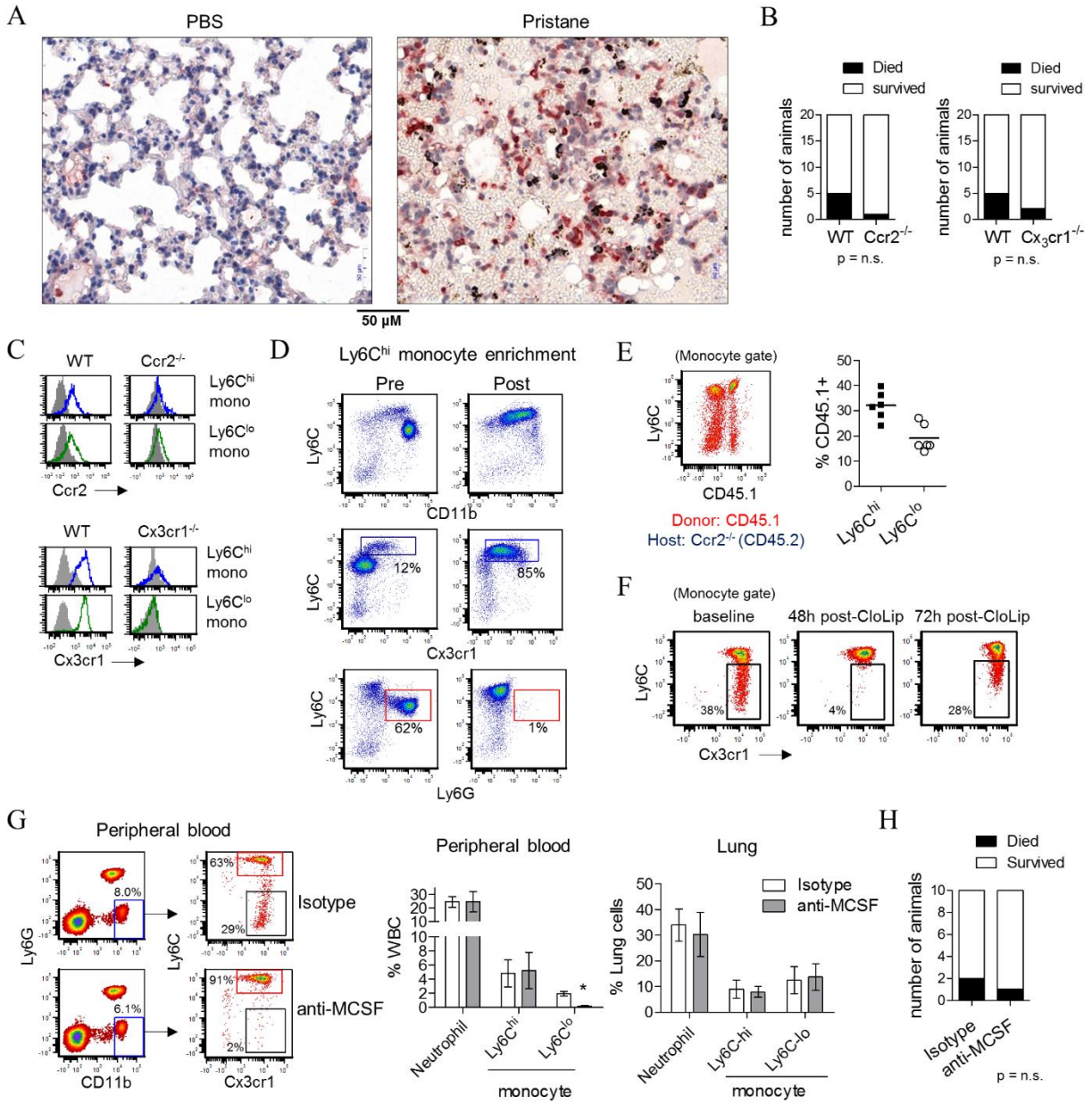


**Supplemental Figure 7. Attenuated DAH in mice deficient of Ccr2 or Cx3cr1.** A) Immunohistochemical staining of Ccl2 in the lung tissue of PBS- or pristane-treated WT mice. B) Mortality rate of Ccr2$^{-/-}$ and Cx3cr1$^{-/-}$ mice (n = 20 per group) two weeks after pristane injection. C) Flow cytometry analysis of Ccr2 and Cx3cr1 expression on lung monocytes from WT, Ccr2$^{-/-}$ and Cx3cr1$^{-/-}$ mice. C) Flow cytometry analysis of bone marrow Ly6C$^{hi}$ monocytes after negative selection using magnetic activated cell sorting. Blue box indicate Ly6C$^{hi}$ monocytes and red box indicate neutrophils. E) Flow cytometry analysis of lung monocytes to discriminate host origin (CD45.2 Ccr2$^{-/-}$) vs. donor origin (CD45.1 SJL) 24 hours after i.v. infusion of Ly6C$^{hi}$ monocytes (n = 6 per group). F) Flow cytometry analysis of lung monocytes before or at indicated time-

points after i.v. treatment with clodronate liposomes. G) Flow cytometry plot and quantification of peripheral blood and lung monocyte populations in pristane-treated mice given anti-MCSF or isotype antibody (n = 10 per group). H) Mortality rate of pristane-treated WT mice given anti-MCSF or isotype antibody. Data are representative of 3 independent experiments (panels A, C, D, F, G) or pooled from 2 to 3 independent experiments (panels B, E, H). Statistical analysis was performed using Fisher's exact test (panels B, H) and unpaired Student's t-test (panel G). * $p < 0.05$